Exact solution of the (0 + 1)-dimensional Boltzmann equation for a massive gas

Wojciech Florkowski
*The H. Niewodniczański Institute of Nuclear Physics, Polish Academy of Sciences, PL-31342 Kraków, Poland
and Institute of Physics, Jan Kochanowski University, PL-25406 Kielce, Poland*

Ewa Maksymiuk
Institute of Physics, Jan Kochanowski University, PL-25406 Kielce, Poland

Radoslaw Ryblewski
*Department of Physics, Kent State University, Kent, Ohio 44242, USA
and The H. Niewodniczański Institute of Nuclear Physics, Polish Academy of Sciences, PL-31342 Kraków, Poland*

Michael Strickland
Department of Physics, Kent State University, Kent, Ohio 44242, USA
(Received 10 March 2014; published 20 May 2014)

We solve the one-dimensional boost-invariant kinetic equation for a relativistic massive system with the collision term treated in the relaxation time approximation. The result is an exact integral equation which can be solved numerically by the method of iteration to arbitrary precision. We compare predictions for the shear and bulk viscosities of a massive system with those obtained from the exact solution. Finally, we compare the time evolution of the bulk pressure obtained from our exact solution with results obtained from the dynamical equations of second-order viscous hydrodynamics.

DOI: 10.1103/PhysRevC.89.054908 PACS number(s): 12.38.Mh, 25.75.−q, 24.10.Nz, 51.10.+y

I. INTRODUCTION

In order to properly understand the data generated in relativistic heavy-ion collisions it is necessary to have dynamical models that can accurately describe the time evolution of the system from the moment after the Lorentz-contracted nuclei pass through one another to the final production of the hadrons that are detected. To date, the primary tool used for describing the time evolution of the matter created in heavy-ion collisions has been relativistic viscous hydrodynamics [1–25]. Originally, most practitioners relied on the Israel–Stewart framework for obtaining the necessary viscous hydrodynamic equations; however, recently there have been efforts to provide more complete formulations of second- and third-order viscous hydrodynamics which should, in principle, more accurately describe the time evolution of the system. In addition to these developments, recently a framework called dissipative anisotropic hydrodynamics has been developed which attempts to improve upon standard relativistic viscous hydrodynamics approximations by relaxing the assumption that the system is approximately isotropic in momentum space [26–38].

If one wants to assess how well these various dissipative relativistic hydrodynamics approaches describe the true nonequilibrium evolution of the system, it is necessary to have some exactly solvable cases that can be used to discriminate the various approaches. One possible avenue for doing this is to compare predictions of hydrodynamic models with exact solutions of the underlying kinetic theory. Doing this in general is not possible; however, there are some cases in which this can be done. Recently it was shown that it was possible to exactly solve the Boltzmann equation in the relaxation time approximation for a system of massless particles which is transversely homogeneous and boost invariant [39,40]. In this paper we generalize the results obtained in Refs. [39,40] to a system of massive particles. This generalization allows us to directly test various predictions available in the literature for the massive near-equilibrium transport coefficients now including bulk viscous effects.

The structure of the paper is as follows: In Sec. II we present the kinetic equation we solve, list the thermodynamic functions for an equilibrium massive Boltzmann gas, specify the boost-invariant variables we will use for the exact solution, and discuss the constraint implied by energy-momentum conservation. In Sec. III we present our exact solution and associated quantities. In Sec. IV we collect results for the shear and bulk viscosities of a massive Boltzmann gas and compute some asymptotic limits of these transport coefficients. In this section we also list three evolution equations for the bulk pressure which can be found in the literature. In Sec. V we present a numerical evaluation of our exact solution and compare the results obtained with the massless limit and various results available from relativistic viscous hydrodynamics. In Sec. VI we briefly discuss the implications of having a fixed shear viscosity to entropy density ratio on the equilibration of the system. Finally, in Sec. VII we conclude and give an outlook for the future.

II. BOLTZMANN EQUATION IN RELAXATION TIME APPROXIMATION

In this paper we consider the relativistic Boltzmann equation

$$p^{\mu}\partial_{\mu} f(x,p) = C[f(x,p)], \tag{1}$$

where $f(x,p)$ is the one-particle distribution function, and C is the collision term which we treat in the relaxation time approximation [41],

$$C[f] = -\frac{p\cdot u}{\tau_{\rm eq}}(f - f_{\rm eq}), \tag{2}$$

where $p\cdot u \equiv p_\mu u^\mu$ and $\tau_{\rm eq}$ is the relaxation time. Herein, we will take the background equilibrium distribution function $f_{\rm eq}$ to be a classical Boltzmann distribution

$$f_{\rm eq} = \frac{2}{(2\pi)^3}\exp\left(-\frac{p\cdot u}{T}\right). \tag{3}$$

However, we note that the results contained herein can be straightforwardly generalized to the case of Bose–Einstein or Fermi–Dirac distributions. The factor of two in Eq. (3) accounts for spin degeneracy. The temperature T is obtained from the Landau matching condition which demands that the energy density calculated from the distribution function f is equal to the energy density obtained from the equilibrium distribution $f_{\rm eq}$. We will provide the details of how this is accomplished in practice below. If the system is close to thermal equilibrium, then T can be interpreted as the true temperature of the system; however, since we consider a nonequilibrium system, T should be interpreted as an effective temperature which is related to the nonequilibrium energy density of the system. The quantity u^μ in Eq. (3) is the flow velocity of matter with $u^\mu_{\rm LRF} = (1,\mathbf{0})$ in the local rest frame (LRF) of the matter.

We note that the simple forms of Eqs. (1)–(3) used herein are motivated in large part by the fact that there are many results which have been obtained with these assumptions and, as a consequence, this allows us to make direct comparisons with other approaches. In particular, we note that there exist several calculations of the relaxation time approximation kinetic coefficients using this setup; see, e.g., Refs. [18,42–47].

A. Equilibrium thermodynamic functions

For massive particles obeying classical Boltzmann statistics the equilibrium particle density, entropy density, energy density, and pressure can be expressed as [48,49]

$$\mathcal{N}_{\rm eq}(T) = \frac{g_0 m^2 T}{\pi^2} K_2\left(\frac{m}{T}\right), \tag{4a}$$

$$\mathcal{S}_{\rm eq}(T) = \frac{g_0 m^2}{\pi^2}\left[4T K_2\left(\frac{m}{T}\right) + m K_1\left(\frac{m}{T}\right)\right], \tag{4b}$$

$$\mathcal{E}_{\rm eq}(T) = \frac{g_0 m^2 T}{\pi^2}\left[3T K_2\left(\frac{m}{T}\right) + m K_1\left(\frac{m}{T}\right)\right], \tag{4c}$$

$$\mathcal{P}_{\rm eq}(T) = \frac{g_0 m^2 T^2}{\pi^2} K_2\left(\frac{m}{T}\right), \tag{4d}$$

where K_n are modified Bessel functions and g_0 is a degeneracy factor which accounts for all internal degrees of freedom except the spin, which we have included separately in Eq. (3).

B. Boost-invariant variables

As mentioned previously, in this paper we consider the case of a transversely homogeneous boost-invariant system. For one-dimensional boost-invariant expansion, all scalar functions of space and time can depend only on the proper time $\tau = (t^2 - z^2)^{1/2}$. In addition, in this case the hydrodynamic flow u^μ should have the Bjorken form in the laboratory frame $u^\mu = (t/\tau, 0, 0, z/\tau)$ [50]. As usual, the phase-space distribution function $f(x,p)$ itself transforms as a scalar under Lorentz transformations. In this case, the requirement of boost invariance implies that $f(x,p)$ can depend only on τ, w, and $\vec{p}_T$ with [51,52]

$$w = t p_L - z E. \tag{5}$$

By using w and p_L one can define another boost-invariant variable:

$$v(\tau, w, p_T) = Et - p_L z = \sqrt{w^2 + \left(m^2 + \vec{p}_T^{\,2}\right)\tau^2}. \tag{6}$$

From Eqs. (5) and (6) one finds the energy and the longitudinal momentum of a particle:

$$E = p^0 = \frac{vt + wz}{\tau^2}, \quad p_L = \frac{wt + vz}{\tau^2}. \tag{7}$$

The momentum-space integration measure can be expressed in terms of these variables as

$$dP = 2d^4p\,\delta(p^2 - m^2)\theta(p^0) = d^2p_T\frac{dp_L}{p^0} = d^2p_T\frac{dw}{v}. \tag{8}$$

Using the boost-invariant variables introduced above, the kinetic equation may be written in the simple form:

$$\frac{\partial f}{\partial \tau} = \frac{f_{\rm eq} - f}{\tau_{\rm eq}}, \tag{9}$$

where the boost-invariant form of the equilibrium distribution function (3) is

$$f_{\rm eq}(\tau, w, p_T) = \frac{2}{(2\pi)^3}\exp\left[-\frac{\sqrt{w^2 + \left(m^2 + p_T^2\right)\tau^2}}{T(\tau)\tau}\right]. \tag{10}$$

Below, we assume that $f(\tau, w, \vec{p}_T)$ is an even function of w and depends only on the magnitude of the transverse momentum $\vec{p}_T$; namely,

$$f(\tau, w, p_T) = f(\tau, -w, p_T). \tag{11}$$

C. Energy-momentum conservation

The energy-momentum tensor can be obtained via

$$T^{\mu\nu}(\tau) = g_0 \int dP\, p^\mu p^\nu f(\tau, w, p_T). \tag{12}$$

By using Eq. (11) one can express the energy-momentum tensor (12) in the form [31,32]

$$T^{\mu\nu} = (\mathcal{E} + \mathcal{P}_T)u^\mu u^\nu - \mathcal{P}_T g^{\mu\nu} + (\mathcal{P}_L - \mathcal{P}_T)z^\mu z^\nu, \tag{13}$$

where the energy density $\mathcal{E}$, the longitudinal pressure $\mathcal{P}_L$, and the transverse pressure $\mathcal{P}_T$, can be obtained via

$$\mathcal{E}(\tau) = \frac{g_0}{\tau^2}\int dP v^2 f(\tau,w,p_T), \tag{14a}$$

$$\mathcal{P}_L(\tau) = \frac{g_0}{\tau^2}\int dP w^2 f(\tau,w,p_T), \tag{14b}$$

$$\mathcal{P}_T(\tau) = \frac{g_0}{2}\int dP p_T^2 f(\tau,w,p_T), \tag{14c}$$

and $z^\mu = (z/\tau,0,0,t/\tau)$ is a four-vector which defines the beam direction. Energy-momentum conservation requires that

$$\partial_\mu T^{\mu\nu} = 0. \tag{15}$$

For a one-dimensional boost-invariant system, the four equations implicit in Eq. (15) reduce to a single equation

$$\frac{d\mathcal{E}}{d\tau} = -\frac{\mathcal{E}+\mathcal{P}_L}{\tau}. \tag{16}$$

We note that the structure of the energy-momentum tensor (13) and the explicit representations given in Eqs. (14) are typical for a momentum-space anisotropic system. The energy conservation equation (15) is satisfied if the energy densities calculated with the nonequilibrium distribution functions f or the equilibrium distribution function $f_{\rm eq}$ are equal, which requires that

$$\begin{aligned}\mathcal{E}(\tau) &= \frac{g_0}{\tau^2}\int dP v^2 f(\tau,w,p_T)\\ &= \frac{g_0}{\tau^2}\int dP v^2 f_{\rm eq}(\tau,w,p_T)\\ &= \frac{g_0 m^2 T}{\pi^2}\left[3T K_2\left(\frac{m}{T}\right) + m K_1\left(\frac{m}{T}\right)\right].\end{aligned} \tag{17}$$

This requirement represents the so-called dynamical Landau matching condition and can be used to define the effective temperature T at any proper time.

III. SOLUTIONS OF KINETIC EQUATION

We now proceed to solve the kinetic equation (1) for a transversely homogenous boost-invariant system.

A. General form of solutions

The general form of solutions of Eq. (1) can be expressed as [39,40,53–56]

$$\begin{aligned}f(\tau,w,p_T) &= D(\tau,\tau_0) f_0(w,p_T)\\ &\quad + \int_{\tau_0}^{\tau}\frac{d\tau'}{\tau_{\rm eq}(\tau')} D(\tau,\tau') f_{\rm eq}(\tau',w,p_T),\end{aligned} \tag{18}$$

where we have introduced the damping function

$$D(\tau_2,\tau_1) = \exp\left[-\int_{\tau_1}^{\tau_2}\frac{d\tau''}{\tau_{\rm eq}(\tau'')}\right]. \tag{19}$$

For the purposes of this paper, we will assume that at $\tau=\tau_0$ the distribution function f can be expressed in Romatschke–Strickland form with an underlying Boltzmann distribution as the isotropic distribution [57]:

$$\begin{aligned}f_0(w,p_T) &= \frac{2}{(2\pi)^3}\exp\left[-\frac{\sqrt{(p\cdot u)^2+\xi_0(p\cdot z)^2}}{\Lambda_0}\right]\\ &= \frac{1}{4\pi^3}\exp\left[-\frac{\sqrt{(1+\xi_0)w^2+\left(m^2+p_T^2\right)\tau_0^2}}{\Lambda_0\tau_0}\right].\end{aligned} \tag{20}$$

This form simplifies to an isotropic Boltzmann distribution if the anisotropy parameter ξ_0 is zero, in which case the transverse momentum scale Λ_0 can be identified with the system's initial temperature T_0.

B. Dynamical Landau matching

By multiplying Eqs. (10) and (20) by $g_0 v^2/\tau^2$ and integrating over momentum one obtains

$$\frac{g_0}{\tau^2}\int dP v^2 f_{\rm eq}(\tau',w,p_T) = \frac{g_0 T^4(\tau')}{2\pi^2}\tilde{\mathcal{H}}_2\left[\frac{\tau'}{\tau},\frac{m}{T(\tau')}\right], \tag{21}$$

$$\frac{g_0}{\tau^2}\int dP v^2 f_0(w,p_T) = \frac{g_0\Lambda_0^4}{2\pi^2}\tilde{\mathcal{H}}_2\left[\frac{\tau_0}{\tau\sqrt{1+\xi_0}},\frac{m}{\Lambda_0}\right], \tag{22}$$

where the function $\tilde{\mathcal{H}}_2(y,z)$ is defined by the integral

$$\tilde{\mathcal{H}}_2(y,z) = \int_0^\infty du\, u^3 \mathcal{H}_2\left(y,\frac{z}{u}\right)\exp(-\sqrt{u^2+z^2}), \tag{23}$$

with

$$\mathcal{H}_2(y,\zeta) = y\int_0^\pi d\phi \sin\phi\sqrt{y^2\cos^2\phi+\sin^2\phi+\zeta^2}. \tag{24}$$

We note that Eqs. (21) and (22) are equal if $\tau=\tau'=\tau_0$ and the system is initially isotropic ($\xi_0=0$). In this case the parameter Λ_0 can be identified with the system's temperature $T(\tau)$ and the expressions on the left-hand sides of Eqs. (21) and (22) become the equilibrium energy density $\mathcal{E}_{\rm eq}(T(\tau))$.

In general, the integral appearing in Eq. (24) can be performed analytically, with the result being

$$\mathcal{H}_2(y,\zeta) = y\left(\sqrt{y^2+\zeta^2} + \frac{1+\zeta^2}{\sqrt{y^2-1}}\tanh^{-1}\sqrt{\frac{y^2-1}{y^2+\zeta^2}}\right). \tag{25}$$

However, the remaining integration over u in Eq. (23) must be performed numerically. We note that the function $\mathcal{H}_2(y,0)$ reduces to the function $\mathcal{H}(y)$ introduced in Ref. [40] and, hence, $\tilde{\mathcal{H}}_2(y,0) = 6\mathcal{H}(y)$.

By using Eqs. (17), (18), (21), and (22) to implement the dynamical Landau matching, we obtain our main result:

$$\begin{aligned}&2m^2 T(\tau)\left[3T(\tau)K_2\left(\frac{m}{T(\tau)}\right) + mK_1\left(\frac{m}{T(\tau)}\right)\right]\\ &= D(\tau,\tau_0)\Lambda_0^4\tilde{\mathcal{H}}_2\left[\frac{\tau_0}{\tau\sqrt{1+\xi_0}},\frac{m}{\Lambda_0}\right]\\ &\quad + \int_{\tau_0}^{\tau}\frac{d\tau'}{\tau_{\rm eq}} D(\tau,\tau') T^4(\tau')\tilde{\mathcal{H}}_2\left[\frac{\tau'}{\tau},\frac{m}{T(\tau')}\right].\end{aligned} \tag{26}$$

This is an integral equation for the effective temperature $T(\tau)$. It can be solved by using the iterative method [58]. In the massless limit ($m \to 0$), Eq. (27) reduces to Eq. (38) of Ref. [40].

C. Transverse and longitudinal pressures

A sensitive measure of the degree of equilibration can be obtained by computing the system's transverse and longitudinal pressures. One can calculate the transverse and longitudinal pressures using Eqs. (14). Similarly to Eqs. (21) and (22) one obtains

$$\frac{g_0}{2}\int dP p_T^2 f_{\rm eq}(\tau',w,p_T) = \frac{g_0 T^4(\tau')}{4\pi^2}\tilde{\mathcal{H}}_{2T}\left[\frac{\tau'}{\tau},\frac{m}{T(\tau')}\right], \quad (27)$$

$$\frac{g_0}{2}\int dP p_T^2 f_0(w,p_T) = \frac{g_0 \Lambda_0^4}{4\pi^2}\tilde{\mathcal{H}}_{2T}\left[\frac{\tau_0}{\tau\sqrt{1+\xi_0}},\frac{m}{\Lambda_0}\right], \quad (28)$$

where we have introduced the new function

$$\tilde{\mathcal{H}}_{2T}(y,z) = \int_0^\infty du u^3 \mathcal{H}_{2T}\left(y,\frac{z}{u}\right)\exp(-\sqrt{u^2+z^2}), \quad (29)$$

with

$$\mathcal{H}_{2T}(y,\zeta) = y\int_0^\pi \frac{d\phi \sin^3\phi}{\sqrt{y^2\cos^2\phi+\sin^2\phi+\zeta^2}} = \frac{y}{(y^2-1)^{3/2}}\left[(\zeta^2+2y^2-1)\tanh^{-1}\sqrt{\frac{y^2-1}{y^2+\zeta^2}} - \sqrt{(y^2-1)(y^2+\zeta^2)}\right]. \quad (30)$$

Equations (27)–(30) allow us to write a compact formula for the transverse pressure:

$$\mathcal{P}_T(\tau) = \frac{g_0}{4\pi^2}D(\tau,\tau_0)\Lambda_0^4\tilde{\mathcal{H}}_{2T}\left[\frac{\tau_0}{\tau\sqrt{1+\xi_0}},\frac{m}{\Lambda_0}\right] + \frac{g_0}{4\pi^2}\int_{\tau_0}^{\tau}\frac{d\tau'}{\tau_{\rm eq}}D(\tau,\tau')T^4(\tau')\tilde{\mathcal{H}}_{2T}\left[\frac{\tau'}{\tau},\frac{m}{T(\tau')}\right]. \quad (31)$$

In order to calculate $\mathcal{P}_T(\tau)$ using Eq. (31), one has to determine the proper-time dependence of $T(\tau)$ by solving the integral equation (26). Once $T(\tau)$ is obtained, the integral over τ' in Eq. (31) can be performed. Similarly to the functions $\tilde{\mathcal{H}}_2(y,z)$ and $\mathcal{H}_2(y,\zeta)$, the functions $\tilde{\mathcal{H}}_{2T}(y,z)$ and $\mathcal{H}_{2T}(y,\zeta)$ satisfy the relations $\mathcal{H}_{2T}(y,0) = \mathcal{H}_T(y)$ and $\tilde{\mathcal{H}}_{2T}(y,0) = 6\mathcal{H}_T(y)$, where $\mathcal{H}_T(y)$ is defined in Ref. [40].

In the case of the longitudinal pressure, one can follow a similar procedure. Once again, one calculates the appropriate moments of the distribution functions

$$\frac{g_0}{\tau^2}\int dP w^2 f_{\rm eq}(\tau',w,p_T) = \frac{g_0 T^4(\tau')}{2\pi^2}\tilde{\mathcal{H}}_{2L}\left[\frac{\tau'}{\tau},\frac{m}{T(\tau')}\right], \quad (32)$$

$$\frac{g_0}{\tau^2}\int dP w^2 f_0(w,p_\perp) = \frac{g_0 \Lambda_0^4}{2\pi^2}\tilde{\mathcal{H}}_{2L}\left[\frac{\tau_0}{\tau\sqrt{1+\xi_0}},\frac{m}{\Lambda_0}\right], \quad (33)$$

where the function $\tilde{\mathcal{H}}_{2L}$ is defined by

$$\tilde{\mathcal{H}}_{2L}(y,z) = \int_0^\infty du u^3 \mathcal{H}_{2L}\left(y,\frac{z}{u}\right)\exp(-\sqrt{u^2+z^2}), \quad (34)$$

with

$$\mathcal{H}_{2L}(y,\zeta) = y^3\int_0^\pi \frac{d\phi \sin\phi\cos^2\phi}{\sqrt{y^2\cos^2\phi+\sin^2\phi+\zeta^2}} = \frac{y^3}{(y^2-1)^{3/2}}\left[\sqrt{(y^2-1)(y^2+\zeta^2)} - (\zeta^2+1)\tanh^{-1}\sqrt{\frac{y^2-1}{y^2+\zeta^2}}\right]. \quad (35)$$

Using Eqs. (32)–(35) one finds

$$\mathcal{P}_L(\tau) = \frac{g_0}{2\pi^2}D(\tau,\tau_0)\Lambda_0^4\tilde{\mathcal{H}}_{2L}\left[\frac{\tau_0}{\tau\sqrt{1+\xi_0}},\frac{m}{\Lambda_0}\right] + \frac{g_0}{2\pi^2}\int_{\tau_0}^{\tau}\frac{d\tau'}{\tau_{\rm eq}}D(\tau,\tau')T^4(\tau')\tilde{\mathcal{H}}_{2L}\left[\frac{\tau'}{\tau},\frac{m}{T(\tau')}\right], \quad (36)$$

where, once again, if the function $T(\tau)$ is known, Eq. (36) can be used to calculate the longitudinal pressure as a function of proper time. As before, one finds that $\mathcal{H}_{2L}(y,0) = \mathcal{H}_L(y)$ and $\tilde{\mathcal{H}}_{2L}(y,0) = 6\mathcal{H}_L(y)$, where $\mathcal{H}_L(y)$ has been defined in Ref. [40].

IV. SHEAR AND BULK VISCOSITIES OF A RELATIVISTIC MASSIVE GAS

In the results section we will compare the results of the exact solution with near-equilibrium expansions provided by first- and second-order viscous hydrodynamics. In preparation for this, in this section we collect formulas for the shear and bulk viscosities of relativistic massive systems and discuss their asymptotic limits.

A. Shear viscosity

The shear viscosity of a classical massive gas in the relaxation time approximation (2) was obtained originally by Anderson and Witting [42]:

$$\eta(T) = \frac{\tau_{\rm eq}P_{\rm eq}(T)}{15}\gamma^3\left[\frac{3}{\gamma^2}\frac{K_3}{K_2} - \frac{1}{\gamma} + \frac{K_1}{K_2} - \frac{K_{i,1}}{K_2}\right], \quad (37)$$

where all functions above are understood to be evaluated at $\gamma \equiv m/T$ and the function $K_{i,1}$ is defined by the integral

$$K_{i,1}(\gamma) = \int_0^\infty \frac{e^{-\gamma\cosh t}}{\cosh t}dt, \quad (38)$$

which can be expressed as

$$K_{i,1}(\gamma) = \frac{\pi}{2}[1-\gamma K_0(\gamma)L_{-1}(\gamma) - \gamma K_1(\gamma)L_0(\gamma)], \quad (39)$$

where L_i is a modified Struve function. Equation (37) gives the proper-time dependence of the shear viscosity coefficient since, using the exact solution, one can determine $T(\tau)$. This result will be compared with the kinetic estimate of the shear viscosity which can be obtained from

$$\eta_{\rm kin}(\tau) = \tfrac{1}{2}\tau(\mathcal{P}_T(\tau) - \mathcal{P}_L(\tau)). \quad (40)$$

The form (40) follows from the structure of the energy-momentum tensor in boost-invariant first-order viscous hydrodynamics. Therefore, one expects that the results obtained using Eqs. (37) and (40) will agree only at late times, $\tau \gg \tau_{\rm eq}$, when the system approaches equilibrium.

Since the temperature goes to zero at large times, proper understanding of the late-time asymptotic behavior of the system requires understanding of the $\gamma \to \infty$ limit of this quantity. In this limit, Eq. (37) becomes

$$\lim_{\gamma\to\infty} \eta = \tau_{\rm eq}\mathcal{P}_{\rm eq} + O(\gamma^{-1}), \tag{41}$$

where we have used the fact that

$$\lim_{\gamma\to\infty} \frac{K_{i,1}}{K_2} = 1 - \frac{5}{2\gamma} + \frac{39}{8\gamma^2} + \frac{45}{8\gamma^3} + \frac{885}{128\gamma^4} + O(\gamma^{-5}). \tag{42}$$

As a consequence, in this limit $\bar{\eta} = \eta/\mathcal{S}_{\rm eq}$ becomes

$$\lim_{\gamma\to\infty} \bar{\eta} \approx \tau_{\rm eq}\frac{\mathcal{P}_{\rm eq}}{\mathcal{S}_{\rm eq}} \approx \tau_{\rm eq}\frac{T^2}{m}. \tag{43}$$

B. Bulk viscosity

The bulk viscosity for a massive Boltzmann gas can be found in Refs. [18,46,47][1]

$$\zeta(T) = \tau_{\rm eq}\frac{g_0 m^2}{3\pi^2 T}\int_0^\infty p^2 e^{-\frac{\sqrt{m^2+p^2}}{T}}\left[c_s^2(T) - \frac{p^2}{3(m^2+p^2)}\right]dp. \tag{44}$$

The integral over momentum in Eq. (44) can be performed, giving

$$\begin{aligned}\zeta(T) &= \tau_{\rm eq}P_{\rm eq}\frac{\gamma^2}{3}\left[\left(c_s^2(T) - \frac{1}{3}\right) + \frac{\gamma}{3}\left(\frac{K_1}{K_2} - \frac{K_{i,1}}{K_2}\right)\right] \\ &= \tau_{\rm eq}P_{\rm eq}\frac{\gamma^2}{3}\left[-\frac{\gamma K_2}{3(3K_3+\gamma K_2)} + \frac{\gamma}{3}\left(\frac{K_1}{K_2} - \frac{K_{i,1}}{K_2}\right)\right].\end{aligned} \tag{45}$$

Since there are similar terms in the expressions for the shear and bulk viscosities (proportional to the difference $K_1 - K_{i,1}$) one may find a relationship between ζ and η; namely,

$$\zeta(T) = \frac{5}{3}\eta(T) - \tau_{\rm eq}P_{\rm eq}\frac{\gamma^3}{9}\left(\frac{K_2}{3K_3+\gamma K_2} + \frac{3K_3}{\gamma^2 K_2} - \frac{1}{\gamma}\right). \tag{46}$$

In the limit of large masses (or, alternatively, low temperatures) one may use Eq. (41) and expand the Bessel functions on the right-hand side of Eq. (46) to obtain

$$\lim_{\gamma\to\infty} \zeta(T) = \tfrac{2}{3}\tau_{\rm eq}P_{\rm eq} + O(\gamma^{-1}). \tag{47}$$

Below, we present the numerical evidence that Eq. (44) and its equivalent forms (45) or (46) are the correct results for the bulk viscosity of a massive system. Our considerations are based on the analysis of the bulk viscous pressure $\Pi_\zeta^{\rm kin}$ which may be obtained directly from our exact solution by computing

$$\Pi_\zeta^{\rm kin}(\tau) = \tfrac{1}{3}[\mathcal{P}_L(\tau) + 2\mathcal{P}_T(\tau) - 3P_{\rm eq}(\tau)]. \tag{48}$$

This expression follows from the energy-momentum tensor used in boost-invariant viscous hydrodynamics and is not restricted to the first-order scheme. Only when the system approaches equilibrium at proper times $\tau \gg \tau_{\rm eq}$ can the bulk viscous pressure be determined by the bulk viscosity $\zeta(T)$ through the relation

$$\Pi_\zeta^{\rm kin}(\tau) \approx -\frac{\zeta(T(\tau))}{\tau}. \tag{49}$$

C. Second-order viscous hydrodynamic equations for bulk viscous pressure

Our exact computation of the bulk viscous pressure can be compared with second-order viscous hydrodynamic predictions for the time dependence of this quantity. Below we consider three possibilities for the evolution equation which appear in the literature:

$$\tau_{\rm eq}\frac{d\Pi_\zeta^{\rm hyd}}{d\tau} + \Pi_\zeta^{\rm hyd} = -\frac{\zeta}{\tau} - \frac{\tau_{\rm eq}\Pi_\zeta^{\rm hyd}}{2}\left(\frac{1}{\tau} - \frac{1}{\zeta}\frac{d\zeta}{d\tau} - \frac{1}{T}\frac{dT}{d\tau}\right), \tag{50}$$

$$\tau_{\rm eq}\frac{d\Pi_\zeta^{\rm hyd}}{d\tau} + \Pi_\zeta^{\rm hyd} = -\frac{\zeta}{\tau} - \frac{4\tau_{\rm eq}\Pi_\zeta^{\rm hyd}}{3\tau}, \tag{51}$$

$$\tau_{\rm eq}\frac{d\Pi_\zeta^{\rm hyd}}{d\tau} + \Pi_\zeta^{\rm hyd} = -\frac{\zeta}{\tau}. \tag{52}$$

These three forms appear in Refs. [4,5], [25], and [5], respectively. The final expression (52) is an approximation to the first expression (50) which is obtained by discarding the second term on the right-hand side. In the subsequent results section we numerically solve Eqs. (50)–(52) using the proper-time dependence of the effective temperature $T(\tau)$ obtained from the exact solution and then compare to the bulk pressure extracted directly from the exact solution using Eq. (48).[2]

V. RESULTS

In this section we present results of our exact solution for a specific initial condition and set of physical parameters. We compare the massless and massive exact solutions to determine what effect the mass has on the evolution of the system. We then compare the shear and bulk viscosities from the literature with those extracted from the exact solution by considering the late-time near-equilibrium evolution of the solutions. Finally, we compare the evolution of the bulk

[1] Anderson and Witting [42] also derived an expression for the bulk viscosity for a massive Boltzmann gas; however, it does not match the result obtained by others. In addition, their expression does not agree with our numerical results at late times, so we do not consider it here.

[2] We have checked explicitly that using the proper-time dependence of the temperature from second-order viscous hydrodynamics yields the same result for the bulk pressure to within a fraction of a percent for the values of $\tau_{\rm eq}$ used herein.

pressure from the exact solution with the evolution predicted by three different viscous hydrodynamics approaches.

A. Initial conditions

We perform our numerical calculations for two fixed values of the initial effective temperature: $T_0 = 600$ MeV and $T_0 = 300$ MeV. The equilibration time τ_{eq} is kept constant and equal to 0.5 fm/c. The integral equation (26) is solved by the iterative method. The initial time is taken to be $\tau_0 = 0.5$ fm/c and we continue the evolution until $\tau = 10$ fm/c. In order to identify the mass effects more clearly, we consider the case of a fixed mass with $m = 300$ MeV.[3] The degeneracy factor g_0 is taken to be 16; however, the specific value of g_0 is irrelevant for our conclusions since it either cancels in ratios we consider or appears as an overall scaling.

The initial distribution function is assumed to be of Romatschke–Strickland form [57] with the initial anisotropy parameter $\xi_0 \in \{0,100\}$, corresponding to an initially isotropic or oblate initial configuration, respectively. The transverse-momentum scale Λ_0 is chosen in such a way that the initial energy density of an anisotropic system coincides with the energy density of an equilibrium system with temperature T_0:

$$2m^2 T_0\left[3T_0 K_2\left(\frac{m}{T_0}\right) + mK_1\left(\frac{m}{T_0}\right)\right] = \Lambda_0^4 \tilde{\mathcal{H}}_2\left[\frac{1}{\sqrt{1+\xi_0}},\frac{m}{\Lambda_0}\right], \tag{53}$$

which is simply the Landau matching condition (27) at $\tau = \tau_0$. We note that for fixed T_0 and ξ_0 the value of Λ_0 depends on m. In the special case $m = 0$, Eq. (53) reduces to the form

$$2T_0^4 = \Lambda_0^4 \mathcal{H}\left(\frac{1}{\sqrt{1+\xi_0}}\right), \tag{54}$$

where, as mentioned previously, $\mathcal{H}$ is defined in Ref. [40].

B. Effective temperature

In Fig. 1 we plot the time dependence of the effective temperature T obtained by iterative solution of Eq. (26). In the top panel we show the results obtained for an initially isotropic system and in the bottom panel we show the case of a highly oblate initial anisotropy. In both the top and bottom panels, the solid lines are the solution for $m = 0$ and the dashed lines are the solution for $m = 300$ MeV. Also, in both the top and bottom panels, the upper set of curves corresponds to $T_0 = 600$ MeV, while the bottom set of curves correspond to $T_0 = 300$ MeV. As we can see from this figure, the primary effect of the mass on the effective temperature is to cause it decrease more slowly as a function of proper time. This behavior is consistent with what one expects from hydrodynamics since, as the mass increases, the speed of sound decreases causing the energy density (and hence the effective temperature) to decrease more slowly as a function of proper time. We also note that the effect of adding a mass is larger for lower initial temperatures, as one would expect based on general arguments.

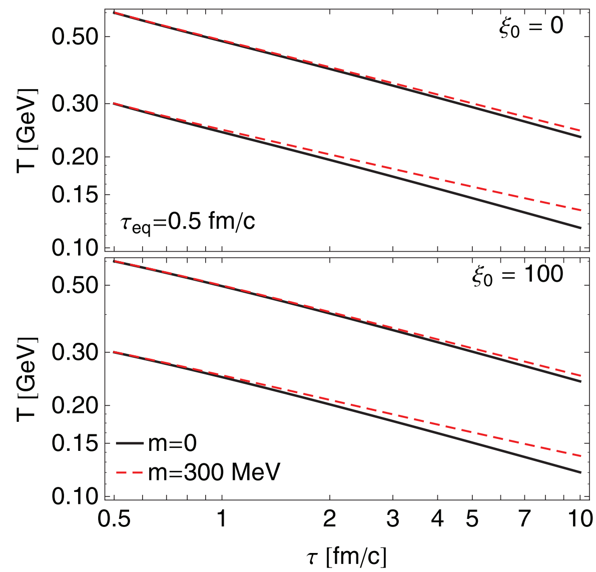

FIG. 1. (Color online) Time dependence of the effective temperature T. Solid lines are the solution for $m = 0$ and dashed lines are the solution for $m = 300$ MeV. In both the top and bottom panels, the upper set of curves corresponds to $T_0 = 600$ MeV, while the bottom set of curves corresponds to $T_0 = 300$ MeV.

C. Pressure anisotropy

In Fig. 2 we plot the time dependence of the ratio of the longitudinal and transverse pressures $\mathcal{P}_L/\mathcal{P}_T$ obtained by using the iterative solution of Eq. (26) to evaluate Eqs. (31)

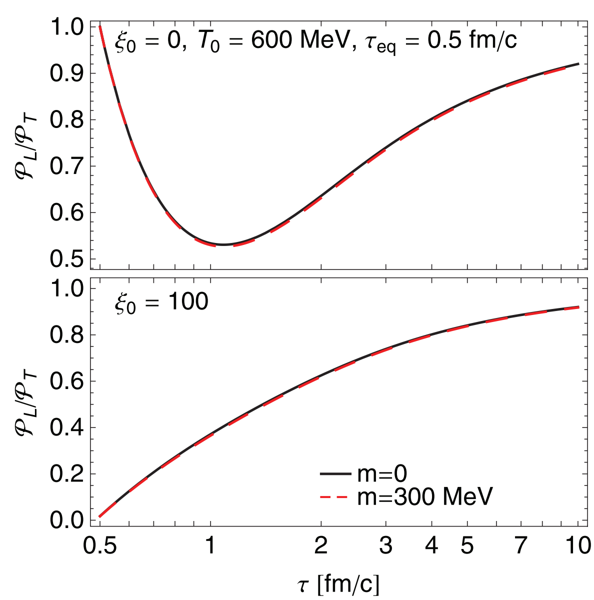

FIG. 2. (Color online) The time dependence of the ratio of the longitudinal and transverse pressures. The initial temperature was taken to be $T_0 = 600$ MeV. The top panel shows the case of an initially isotropic system and the bottom panel shows the case of an initially oblate system.

[3] In the context of quasiparticle models which assume a gluon mass $m_g \sim gT$, with $g \sim 2$ at phenomenologically relevant temperatures, such a mass might even be a bit small.

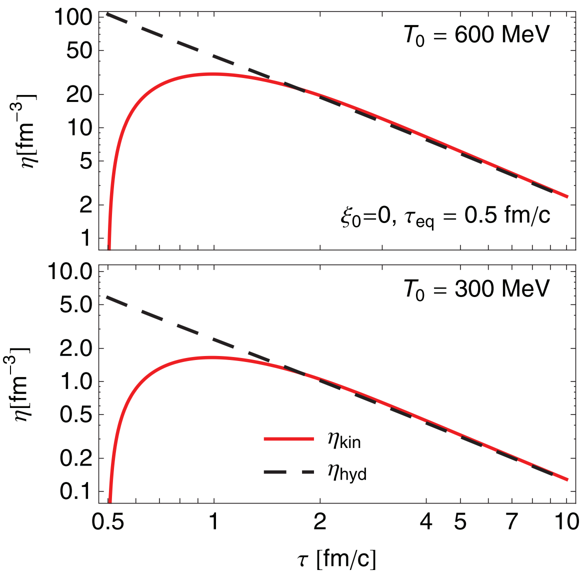

FIG. 3. (Color online) The effective shear viscosity η_{kin} (solid line) compared with η_{hyd} (dashed line) obtained from Eq. (37). The system was assumed to be initially isotropic, i.e., $\xi_0 = 0$. The top panel shows the results obtained for $T_0 = 600$ MeV and the bottom panel shows the results obtained for $T_0 = 300$ MeV.

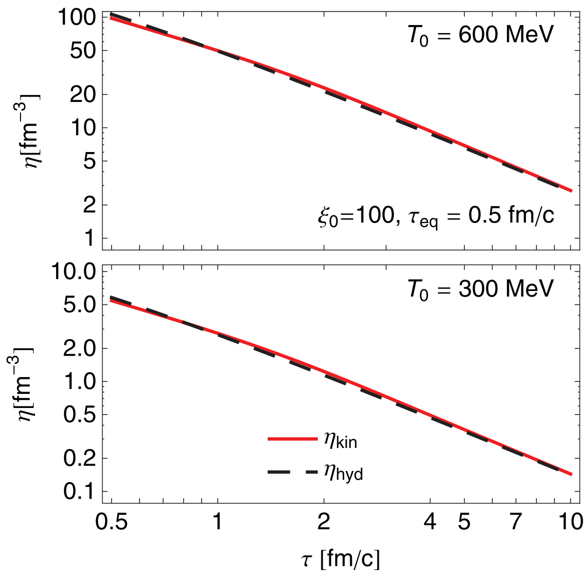

FIG. 4. (Color online) Same as Fig. 3 except with $\xi_0 = 100$.

and (36). The initial temperature was taken to be $T_0 = 600$ MeV; however, we note that this ratio depends very weakly on the initial temperature when the relaxation time is a constant. In the top panel of Fig. 2 we show the case of an initially isotropic system and in the bottom panel we show the case of an initially oblate system. As before, the solid lines are the solution for $m = 0$ and the dashed lines are the solution for $m = 300$ MeV. As we can see from these figures, having a nonzero mass seems to have very little effect on the pressure anisotropy.

D. Shear viscosity

We now turn to a comparison of the effective shear viscosity extracted from our exact solution using Eq. (40) with the near-equilibrium behavior predicted by viscous hydrodynamics. In Figs. 3 and 4 we plot the resulting η_{kin} compared with η_{hyd} obtained from Eq. (37). Figure 3 shows the case $\xi_0 = 0$ and Fig. 4 shows the case $\xi_0 = 100$. In both figures the top panel shows the results obtained for $T_0 = 600$ MeV and the bottom panel shows the results obtained for $T_0 = 300$ MeV. As we can see from these figures, after some initial transient nonequilibrium evolution during which the effective shear viscosity deviates from the near-equilibrium value, the results converge and the exact solution is well approximated by the near-equilibrium shear viscosity (37).

E. Bulk viscosity and pressure

We now turn to the comparison of the proper-time dependence of the bulk pressure and associated bulk viscosity extracted from our exact solution using Eq. (48). In Figs. 5–8 we plot the bulk pressure times τ for five different cases. The solid line is the result obtained using the exact solution and Eq. (48). The other curves shown correspond to the first-order solution (49) indicated by a thick dashed line and the solutions to Eqs. (50), (51), and (52) indicated by a thin dashed line, a dot-dashed line, and a dotted line, respectively. As we can see from these figures, the exact solution and all second-order viscous hydrodynamics variations tend toward the first-order solution at late times. However, none of the second-order viscous hydrodynamics variations seems to accurately describe the early time evolution of the bulk viscous pressure in all cases. Paradoxically, the simple approximate form (52) seems to provide the best approximation when the system initially possesses a highly oblate momentum-space anisotropy; however, it provides the worst approximation if the system is initially isotropic in momentum space. These results indicate that there may be something incomplete in the manner in which second-order viscous hydrodynamics treats the bulk

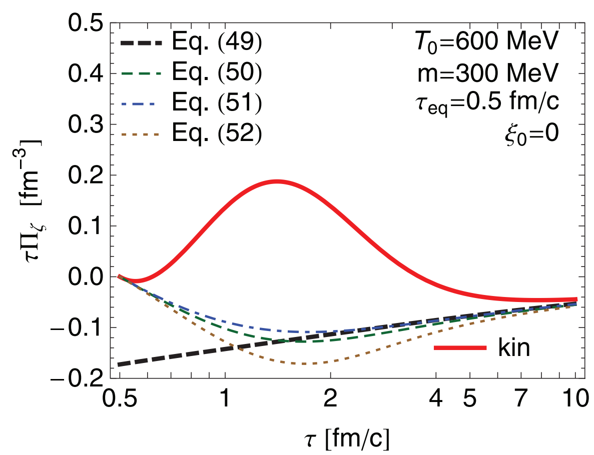

FIG. 5. (Color online) Proper-time dependence of the bulk pressure times τ for $\xi_0 = 0$ and $T_0 = 600$ MeV. Solid line is the exact solution obtained from Eq. (48). The other curves correspond to the first-order solution (49) and the solutions of Eqs. (50), (51), and (52).

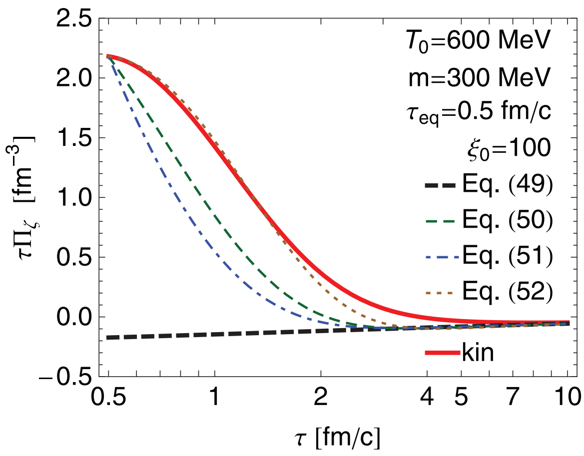

FIG. 6. (Color online) Same as Fig. 5 except with $\xi_0 = 100$.

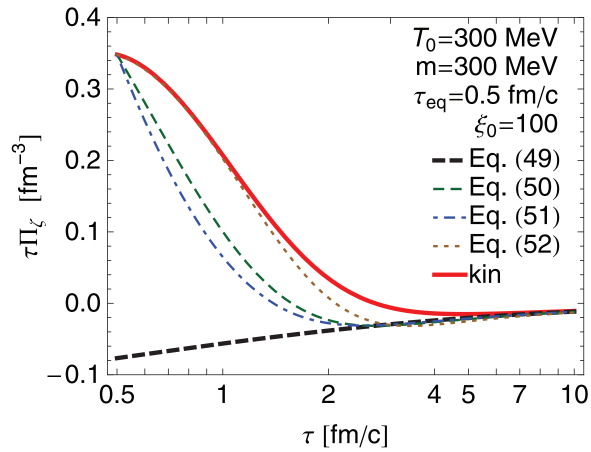

FIG. 8. (Color online) Same as Fig. 5 except with $T_0 = 300$ MeV and $\xi_0 = 100$.

pressure. One possibility is that the evolution equations for the bulk pressure used herein have neglected to include the possibility of shear-bulk coupling which appears, for example, in the complete expansion derived in Ref. [23].

VI. TEMPERATURE-DEPENDENT RELAXATION TIME

Before concluding, we would like to point out that in the previous section we considered numerical results obtained using a time-independent relaxation time τ_{eq}; however, our exact solution (26) is not limited to this case. If one wanted to study the case, for example, that the ratio of the shear viscosity to entropy density were held fixed, this would imply a temperature-dependent, and hence time-dependent, relaxation time. For general masses one could use Eq. (37) expressed in terms of $\bar{\eta} = \eta/S_{eq}$ and then solve for τ_{eq} as function of the mass and temperature. If this were done, one would find that the relaxation time depends nontrivially on the assumed mass. The relation becomes particularly transparent in the limit of large masses, in which case one can use the asymptotic form (43) to obtain $\lim_{\gamma\to\infty} \tau_{eq} = m\bar{\eta}/T^2$, which implies that, for fixed temperature, the relaxation time goes to infinity. In practice, this means that for a massive system one will see larger deviations from equilibrium than for a massless system if one fixes $\bar{\eta}$ and compares the two.

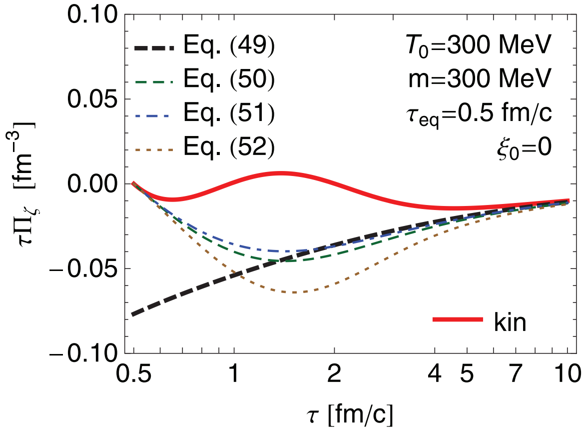

FIG. 7. (Color online) Same as Fig. 5 except with $T_0 = 300$ MeV.

VII. CONCLUSIONS

In this paper we generalized the results of Refs. [39,40] to a system of massive particles obeying Boltzmann statistics. Our main result is an integral equation (26) that can be solved to arbitrary numerical precision by using the method of iteration. Based on this solution one can obtain the proper-time dependence of the full one-particle distribution function and, as a consequence, one can numerically obtain all thermodynamic functions to arbitrary numerical precision. We presented explicit expressions for the transverse pressure (31) and longitudinal pressure (36). We then presented the results of numerical solution of the integral equation for the effective temperature, the pressure anisotropy, the effective shear viscosity, and the bulk pressure. We found that the effect of finite masses on the effective temperature is to cause it to decrease more slowly in proper time, which is consistent with hydrodynamic expectations. We found that the pressure anisotropy depends very weakly on the mass in the case that τ_{eq} is assumed to be independent of the temperature. Finally, we compared our exact results with results obtained from relativistic hydrodynamics. We found that the standard expressions available in the literature for the mass and temperature dependence of the shear and bulk viscosities correctly describe the evolution of the system well for $\tau \gg \tau_{eq}$.

Looking forward it will be interesting to compare results obtained by using anisotropic hydrodynamics for the massive case with the exact solution obtained herein. There are now two formulations of leading-order anisotropic hydrodynamics on the market: one which uses the zeroth moment of the Boltzmann equation to obtain an equation of motion [27] and one which uses the second moment of the Boltzmann equation to obtain an equation of motion [37]. The exact solution continued here can be used to determine which scheme provides the best approximation. We leave this for future work [59].

ACKNOWLEDGMENTS

We thank M. Martinez for discussions. R.R. was supported by Polish National Science Center grant No. DEC-2012/07/D/ST2/02125, the Foundation for Polish Science, and US DOE Grant No. DE-SC0004104. W.F. and E.M. were supported by Polish National Science Center Grant No. DEC-2012/06/A/ST2/00390. M.S. was supported in part by US DOE Grant No. DE-SC0004104.

[1] W. Israel, Ann. Phys. (NY) **100**, 310 (1976).
[2] W. Israel and J. M. Stewart, Ann. Phys. (NY) **118**, 341 (1979).
[3] A. Muronga, Phys. Rev. Lett. **88**, 062302 (2002).
[4] A. Muronga, Phys. Rev. C **69**, 034903 (2004).
[5] U. W. Heinz, H. Song, and A. K. Chaudhuri, Phys. Rev. C **73**, 034904 (2006).
[6] R. Baier, P. Romatschke, and U. A. Wiedemann, Phys. Rev. C **73**, 064903 (2006).
[7] R. Baier, P. Romatschke, D. T. Son, A. O. Starinets, and M. A. Stephanov, J. High Energy Phys. 04 (2008) 100.
[8] P. Romatschke and U. Romatschke, Phys. Rev. Lett. **99**, 172301 (2007).
[9] K. Dusling and D. Teaney, Phys. Rev. C **77**, 034905 (2008).
[10] M. Luzum and P. Romatschke, Phys. Rev. C **78**, 034915 (2008).
[11] H. Song and U. W. Heinz, J. Phys. G **36**, 064033 (2009).
[12] A. El, Z. Xu, and C. Greiner, Phys. Rev. C **81**, 041901 (2010).
[13] J. Peralta-Ramos and E. Calzetta, Phys. Rev. C **82**, 054905 (2010).
[14] G. Denicol, T. Kodama, and T. Koide, J. Phys. G **37**, 094040 (2010).
[15] G. S. Denicol, T. Koide, and D. H. Rischke, Phys. Rev. Lett. **105**, 162501 (2010).
[16] B. Schenke, S. Jeon, and C. Gale, Phys. Rev. Lett. **106**, 042301 (2011).
[17] B. Schenke, S. Jeon, and C. Gale, Phys. Lett. B **702**, 59 (2011).
[18] P. Bozek, Phys. Rev. C **81**, 034909 (2010).
[19] P. Bozek, Phys. Lett. B **699**, 283 (2011).
[20] H. Niemi, G. S. Denicol, P. Huovinen, E. Molnar, and D. H. Rischke, Phys. Rev. Lett. **106**, 212302 (2011).
[21] H. Niemi, G. S. Denicol, P. Huovinen, E. Molnár, and D. H. Rischke, Phys. Rev. C **86**, 014909 (2012).
[22] P. Bożek and I. Wyskiel-Piekarska, Phys. Rev. C **85**, 064915 (2012).
[23] G. S. Denicol, H. Niemi, E. Molnár, and D. H. Rischke, Phys. Rev. D **85**, 114047 (2012).
[24] J. Peralta-Ramos and E. Calzetta, Phys. Rev. D **87**, 034003 (2013).
[25] A. Jaiswal, Phys. Rev. C **87**, 051901 (2013).
[26] W. Florkowski and R. Ryblewski, Phys. Rev. C **83**, 034907 (2011).
[27] M. Martinez and M. Strickland, Nucl. Phys. A **848**, 183 (2010).
[28] R. Ryblewski and W. Florkowski, J. Phys. G **38**, 015104 (2011).
[29] M. Martinez and M. Strickland, Nucl. Phys. A **856**, 68 (2011).
[30] R. Ryblewski and W. Florkowski, Eur. Phys. J. C **71**, 1761 (2011).
[31] W. Florkowski and R. Ryblewski, Phys. Rev. C **85**, 044902 (2012).
[32] M. Martinez, R. Ryblewski, and M. Strickland, Phys. Rev. C **85**, 064913 (2012).
[33] R. Ryblewski and W. Florkowski, Phys. Rev. C **85**, 064901 (2012).
[34] W. Florkowski, R. Maj, R. Ryblewski, and M. Strickland, Phys. Rev. C **87**, 034914 (2013).
[35] W. Florkowski and R. Maj, Acta Phys. Pol., B **44**, 2003 (2013).
[36] D. Bazow, U. W. Heinz, and M. Strickland, arXiv:1311.6720.
[37] L. Tinti and W. Florkowski, Phys. Rev. C **89**, 034907 (2014).
[38] W. Florkowski and O. Madetko, arXiv:1402.2401.
[39] W. Florkowski, R. Ryblewski, and M. Strickland, Nucl. Phys. A **916**, 249 (2013).
[40] W. Florkowski, R. Ryblewski, and M. Strickland, Phys. Rev. C **88**, 024903 (2013).
[41] P. L. Bhatnagar, E. P. Gross, and M. Krook, Phys. Rev. **94**, 511 (1954).
[42] J. Anderson and H. Witting, Physica **74**, 466 (1974).
[43] W. Czyż and W. Florkowski, Acta Phys. Polon., B **17**, 819 (1986).
[44] A. Dyrek and W. Florkowski, Phys. Rev. D **36**, 2172 (1987).
[45] C. Cercignani and G. Kremer, *The Relativistic Boltzmann Equation: Theory and Applications*, Progress in Mathematical Physics (Springer Verlag, New York, 2002).
[46] C. Sasaki and K. Redlich, Phys. Rev. C **79**, 055207 (2009).
[47] P. Romatschke, Phys. Rev. D **85**, 065012 (2012).
[48] S. R. de Groot, W. A. van Leewen, and C. G. van Weert, *Relativistic Kinetic Theory: Principles and Applications* (Elsevier North-Holland, 1980).
[49] W. Florkowski, *Phenomenology of Ultra-Relativistic Heavy-Ion Collisions* (World Scientific, Singapore, 2010).
[50] J. D. Bjorken, Phys. Rev. D **27**, 140 (1983).
[51] A. Białas and W. Czyż, Phys. Rev. D **30**, 2371 (1984).
[52] A. Białas and W. Czyż, Nucl. Phys. B **296**, 611 (1988).
[53] G. Baym, Phys. Lett. B **138**, 18 (1984).
[54] G. Baym, Nucl. Phys. A **418**, 525 (1984).
[55] H. Heiselberg and X.-N. Wang, Phys. Rev. C **53**, 1892 (1996).
[56] S. M. H. Wong, Phys. Rev. C **54**, 2588 (1996).
[57] P. Romatschke and M. Strickland, Phys. Rev. D **68**, 036004 (2003).
[58] B. Banerjee, R. Bhalerao, and V. Ravishankar, Phys. Lett. B **224**, 16 (1989).
[59] W. Florkowski, R. Ryblewski, M. Strickland, and L. Tinti, Phys. Rev. C **89**, 054909 (2014).